1997

Morphology of silica aerogels obtained from the process catalyzed by NH4F and NH4OH

Janusz J. Malinowski
J. Mrowiec-Bialon
L. Pajak
A. B. Jarzebski
A. I. Lachowski

Morphology of Silica Aerogels Obtained from the Process Catalyzed by NH_4F and NH_4OH

Julita Mrowiec-Białoń,[†] Lucjan Pająk,[‡] Andrzej B. Jarzębski,*[,†,§] Andrzej I. Lachowski,[†] and Janusz J. Malinowski[†]

Institute of Chemical Engineering, Polish Academy of Sciences, Bałtycka 5, PL-44101 Gliwice, Poland, Silesian University, Institute of Physics and Chemistry of Metals, Bankowa 12, 40-007 Katowice, Poland, and Silesian Technical University, Department of Chemical Engineering, M. Strzody 7, 44-100 Gliwice, Poland

Received April 2, 1997. In Final Form: August 20, 1997[⊗]

Twelve samples of silica aerogels were synthesized using different concentrations of catalysts (NH_4F, NH_4OH), and their morphology was investigated by means of small-angle X-ray scattering (SAXS), N_2 adsorption, and transmission electron microscopy. Both SAXS and the nitrogen adsorption method consistently show a different influence of the catalysts; fluoride anions promote formation of a tenuous branched-polymeric structure, with mass fractal dimension $D_m \simeq 2.3-2.5$, while addition of hydroxyl ions results in a sparser structure ($D_m \simeq 2.1-2.2$) self-similar over a narrower range. The morphology of aerogels obtained from the process catalyzed by fluoride hydroxide resembles that of aerogels produced by the two-step method. This may suggest similar mechanisms of gel formation in both processes, and, consequently, a dramatic acceleration of the hydrolysis reaction caused by NH_4F.

1. Introduction

Sol-gel silicas doped with activating compound have attracted much attention; an excellent account of the more recent trends and achievements is available.[1] Properties of final materials markedly depend on the effective entrapment of host molecules in silica matrices formed in the process of gelation. Thus this stage of the manufacturing process should be carefully controlled. The rate of gelation in a typical silica sol-gel system: $Si(OR)_4/ROH/H_2O$ is very low and needs to be increased for practical purposes by the use of catalysts. Ammonium hydroxide is perhaps the most common basic catalyst employed in the synthesis of alcogels, but in spite of its use, the gelation time in the single-step and two-step polymerization protocols is counted in hours or even days. The fluoride catalysts (NaF, NH_4F, HF) are known for their ability for boosting gelation and reduce its time to minutes;[2−4] the mixed system comprising NH_4F and NH_4OH also exhibits the same effect.[5] The shortening of gelation is of appreciable advantage for practical purposes, e.g. for the preparation of monolithic silica aerogels[6] and xerogel/aerogel biocatalysts.[7−9] For this reason fluoride anion catalysts have attracted interest, despite their strong toxicity, which obviously has to be taken into account in practical situations. However, the question of the influence of F^- ions on the alcogel/aerogel morphology has as yet proved elusive. Indeed, extensive investigations carried out in the eighties by Rabinovich et al.[4,10] focused mainly on the mechanisms of fluoride ion operation in a silanol environment and less on xerogel texture. Only very recently several papers reported on the effect of reactant concentration on the porous texture of aerogels obtained from the process catalyzed by NH_4F[6,11] or the two-component system of NH_4F and NH_4OH.[12,13] The mechanism of fluoride anion operation is still not entirely clear,[14a] and hence it can hardly facilitate prediction of the F^- concentration influence on the resulting gels' morphology. Experimental evaluation of this effect is the

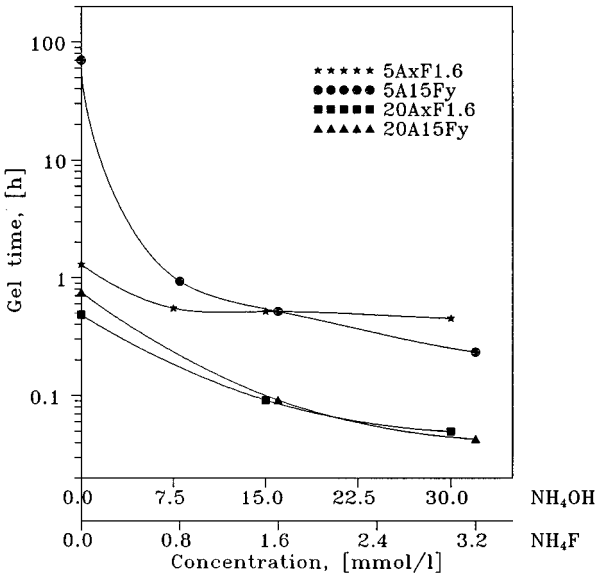

Figure 1. Gelation times versus concentration of the catalyst. The solid lines are a guide to the eye.

* Corresponding author. Telephone: +48−32 310 811. Telefax: +48-32 310 318. E-mail: a.jarzeb@iich.gliwice.pl.
† Polish Academy of Sciences.
‡ Silesian University.
§ Silesian Technical University.
⊗ Abstract published in *Advance ACS Abstracts,* October 1, 1997.

(1) Avnir, D. *Acc. Chem. Res.* **1995**, *28*, 328.
(2) Iler, R. K. *The Chemistry of Silica*; Wiley: New York, 1979; p 212.
(3) Pope, E. J. A.; Mackenzie, J. D. *J. Non-Cryst. Solids* **1986**, *87*, 185.
(4) Rabinovich, E. M.; Nassau, K.; Miller, A. E.; Gallagher, P. K. *J. Non-Cryst. Solids* **1988**, *104*, 107.
(5) Tewari, P. H.; Hunt, A. J.; Lieber, J. G.; Lofftus, K. In *Aerogels*; Fricke, J., Ed.; Springer-Verlag: Berlin, 1986; p 142.
(6) Pajonk, G. M.; Elaloui, E.; Achard, P.; Chevalier, B.; Chevalier, J.-L.; Durant, M. *J. Non-Cryst. Solids* **1995**, *186*, 1.
(7) Reetz, T. M.; Zonta, A.; Simpelkamp, J. *Biotechnol. Bioeng.* **1996**, *49*, 527.
(8) Antczak, T.; Mrowiec-Białoń, J.; Bielecki, S.; Jarzębski, A. B.; Malinowski, J.J.; Lachowski, A. I.; Galas, E. *Biotechnol. Tech.* **1997**, *11*, 9.
(9) Avnir, D.; Braun, S.; Lev, O.; Ottolenghi, M. *Chem. Mater.* **1994**, *6*, 1605.
(10) Wood, D. L.; Rabinovich, E. M. *J. Non-Cryst. Solids* **1986**, *82*, 171.
(11) Ehrburger-Dolle, F.; Dallamano, J.; Elaloui, E.; Pajonk, G. M. *J. Non-Cryst. Solids* **1995**, *186*, 9.
(12) Jarzębski, A. B.; Lorenc, J. *Chem. Eng. Sci.* **1995**, *50*, 357.
(13) Jarzębski, A. B.; Lorenc, J.; Pająk, L. *Langmuir* **1997**, *13*, 1280.
(14) (a) Brinker, C. J.; Scherer, G. W. *Sol-Gel Science*; Academic Press, Inc.: San Diego, CA, 1990; p 119 and (b) p 325.

S0743-7463(97)00345-4 CCC: $14.00

Table 1. Characteristic Parameters of the Silica Aerogels

sample	V_{pN_2} (cm³/g)	ρ_a (g/cm³)	S_{BET} (m²/g)	S_{SAXS} (m²/g)	I_m (Å)	$D_{s(FHH)}$	$D_{m(SAXS)}$
S05A0F1.6	3.0	0.034	770	1026	23	2.53	2.50
S05A7.5F1.6	2.9	0.032	796	922	25	2.57	2.30
S05A15F1.6	3.7	0.032	842	862	27	2.55	2.25
S05A30F1.6	3.6	n.a.	741	881	26	2.54	2.05
S05A15F0	2.4	n.a.	757	874	26	2.66	2.15
S05A15F0.8	2.7	0.034	743	767	30	2.59	2.25
S05A15F3.2	3.1	n.a.	725	762	30	2.55	2.20
S20A0F1.6	3.2	0.063	650	687	26	2.61	2.25
S20A15F1.6	3.4	0.067	663	674	27	2.61	2.15
S20A30F1.6	5.0	n.a.	665	707	26	2.61	2.05
S20A15F0	5.2	0.064	660	689	26	2.61	2.15
S20A15F3.2	4.7	n.a.	762	807	23	2.61	2.10

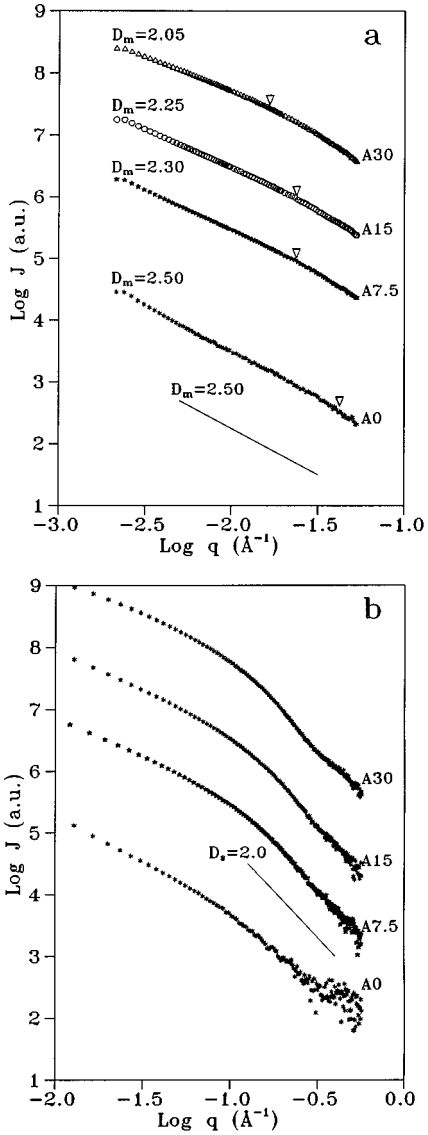

Figure 2. Log−log plot of the scattered intensity from the samples of the S05A*x*F1.6 series. The numbers in the labels are concentrations of NH_4OH (A) in mmol/L.

issue tackled in the current work. To the best of our knowledge no such data have as yet been reported. The series of silica aerogel samples prepared using different concentrations of fluoride anions was probed by means of the small-angle X-ray scattering method (SAXS), nitrogen adsorption/desorption at 77 K, and transmission electron microscopy (TEM). Analysis of structure portrayals provided by these three fundamentally different techniques may also give further vital evidence on the coherence or consistency of predictions provided by these methods.

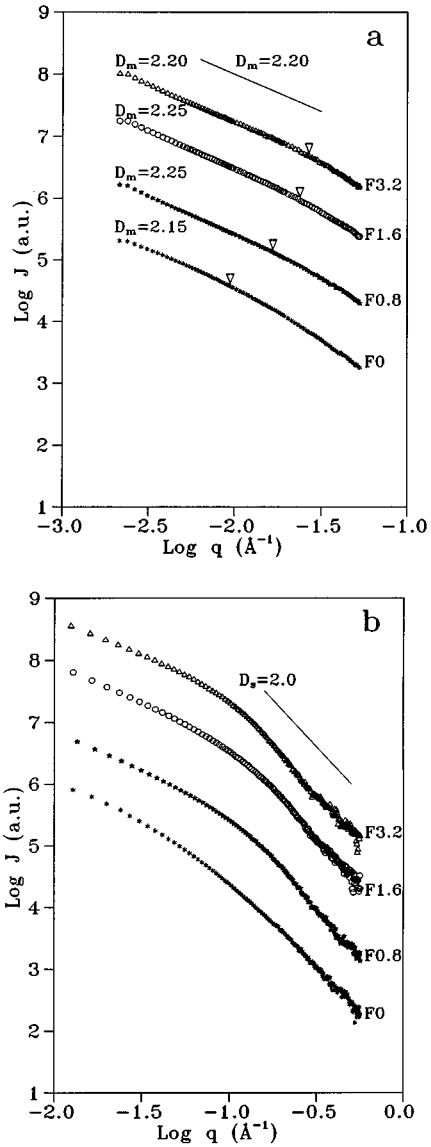

Figure 3. Log−log plot of the scattered intensity from the samples of the S05A15F*y* series. The numbers in the labels are concentrations of NH_4F (F) in mmol/L.

2. Experimental details

Alcogel samples were synthesized in test tubes at 37 °C using tetraethoxysilane (TEOS), ethanol, and water and a complex catalyst system comprising ammonium fluoride and ammonium hydroxide. Twelve alcogel samples were prepared, as given in the general code SAF in Table 1, with the volumetric concentration of TEOS (S) in the EtOH/TEOS system equal to 5 and 20%, respectively, and the water/TEOS molar ratio equal to 4. The concentration of NH_4OH (A) took the values, respectively, 0, 7.5, 15, and 30 mmol/L while that of NH_4F (F) was equal to 0, 0.8, 1.6, or 3.2 mmol/L. The gelation time t_G was checked on tilting the tube and determining the moment when no fluidity was observed. After they were aged for 6 days, the alcogel samples were dried (each S series separately) in a 1 L autoclave at 25 MPa and 300 °C to obtain dry aerogels. The process of drying followed the procedure of van Lierop et al.;[15] i.e., prior to heating, the autoclave was pressurized with 8 MPa of nitrogen. The pore size distribution, specific surface area, S_{BET}, and mesopore volume, V_{pN_2}, were determined from nitrogen adsorption/

(15) van Lierop, J. G.; Huizing, A.; Meerman, W. C. P. M.; Mulder, C. A. M. *J. Non-Cryst. Solids* **1986**, *82*, 265.

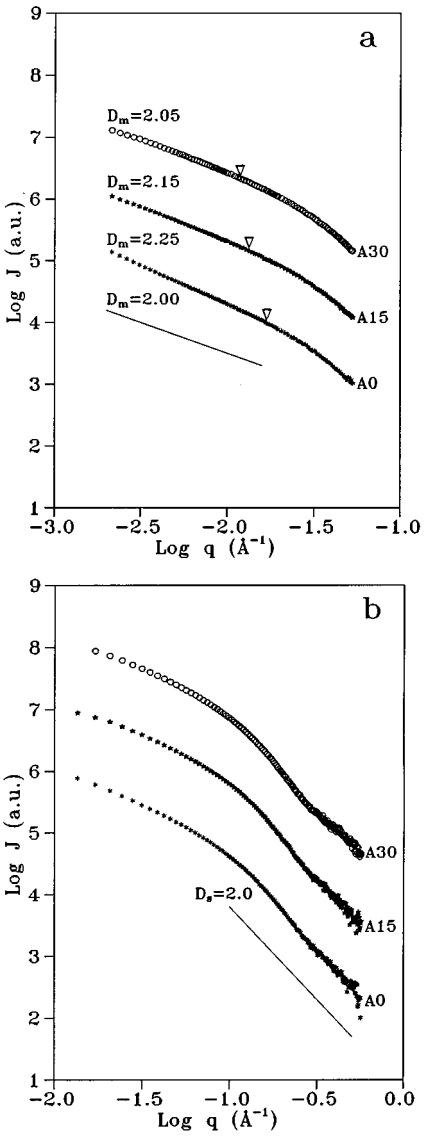

Figure 4. Log−log plot of the scattered intensity from the samples of the S20A*x*F1.6 series. The numbers in the labels are concentrations of NH_4OH (A) in mmol/L.

desorption isotherms measured using a Micromeritics ASAP 2000 instrument, and apparent density, ρ_a, was determined from mercury porosimetry data (Micromeritics Auto Pore 9220). The results obtained are given in Table 1.

SAXS measurements were performed using a Kratky camera, and similarly as before,[12] to obtain a broad range of the scattering vector **q**, two different radiations were used, i.e. Co Kα and Cu Kα, together with two different sets of slits. This made it possible to cover the interval in **q** between 0.0025 and 0.115 Å^{-1}. The samples investigated were granules loosely packed between thin foils. The volume and weight of the material in the cell were carefully noted to give the mass density of the samples. To obtain a desmeared power-law scattering exponent, a 1 was added to the actual exponent ensuing from the experimental scattering curve.

Transmission electron micrographs were obtained on a JEOL 2000SX instrument operating at 160 kV. The aerogel samples were dried for 2 h at 200 °C and subsequently ground to a size of about 60−100 mesh, and the particles were suspended in ethanol and sonicated for 1−2 min. The solution was allowed to settle for 5 min, and a droplet of the resulting supernatant was placed on a holey carbon film and dried.

3. Results and Discussion

As can be seen from Figure 1 fluoride anions dramatically shorten the process of gelation, and this reduction

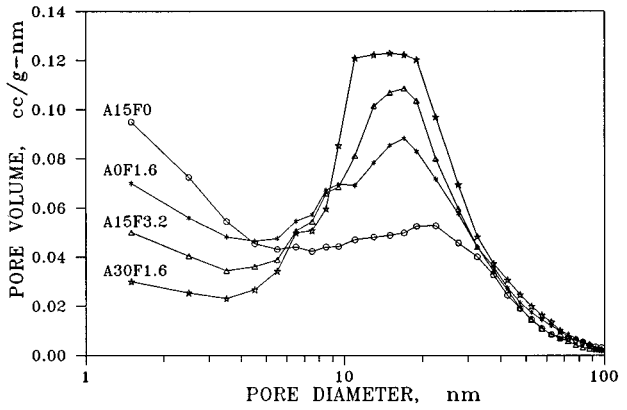

Figure 5. Pore size distribution for four aerogels of the S05 series.

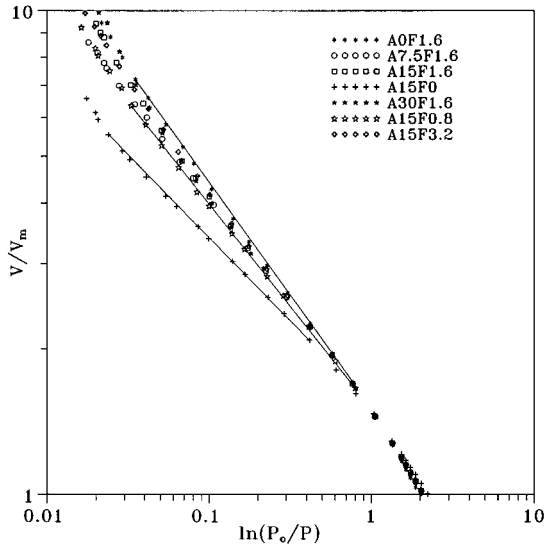

Figure 6. FHH plot of nitrogen adsorption isotherms from the samples of the S05 series.

is more pronounced than that affected by hydroxyl ions, especially at low silica content. The apparent densities of the samples with the same TEOS content were in the range 0.032−0.034 and 0.062−0.065 g/cm^3 for samples of the S05 and S20 series, respectively. Thus, the concentration of the catalyst appears to have little influence on the macrostructure of silica aerogels. The nanostructure of the samples 'seen' by SAXS, N_2 adsorption, and TEM is portrayed in Figures 2−7. The scattering curves obtained using Co Kα filtered radiations are presented in parts a and b of Figures 2−4, and the corresponding pore size distributions (PSDs) and TEM images of representative samples are given in Figures 5 and 7.

The intensities from the samples were analyzed using conventional equations,[16] with the smooth surface assumption (due to well-defined Porod behavior in the short scales) to obtain the values of the specific area S_{SAXS} and of the mean chord length in the solid phase, l_m, given in Table 1. Figures 2 and 3 demonstrate a strong effect of the type of catalyst and its concentration on the morphology and surface structure of the samples. All curves from samples S05A*x*F*y* ($x, y \neq 0$) in the high-**q** region (short scales) exhibit Porod law scattering (from smooth particles) and a positive departure from this law with a decrease in **q**; such behavior is not observed in S05 samples catalyzed either by fluoride or hydroxide anions (cf., curves A0 and F0 in Figures 2b and 3b). Indeed, the magnitude of a

(16) Bota, A. *J. Appl. Crystallogr.* **1991**, *24*, 635.

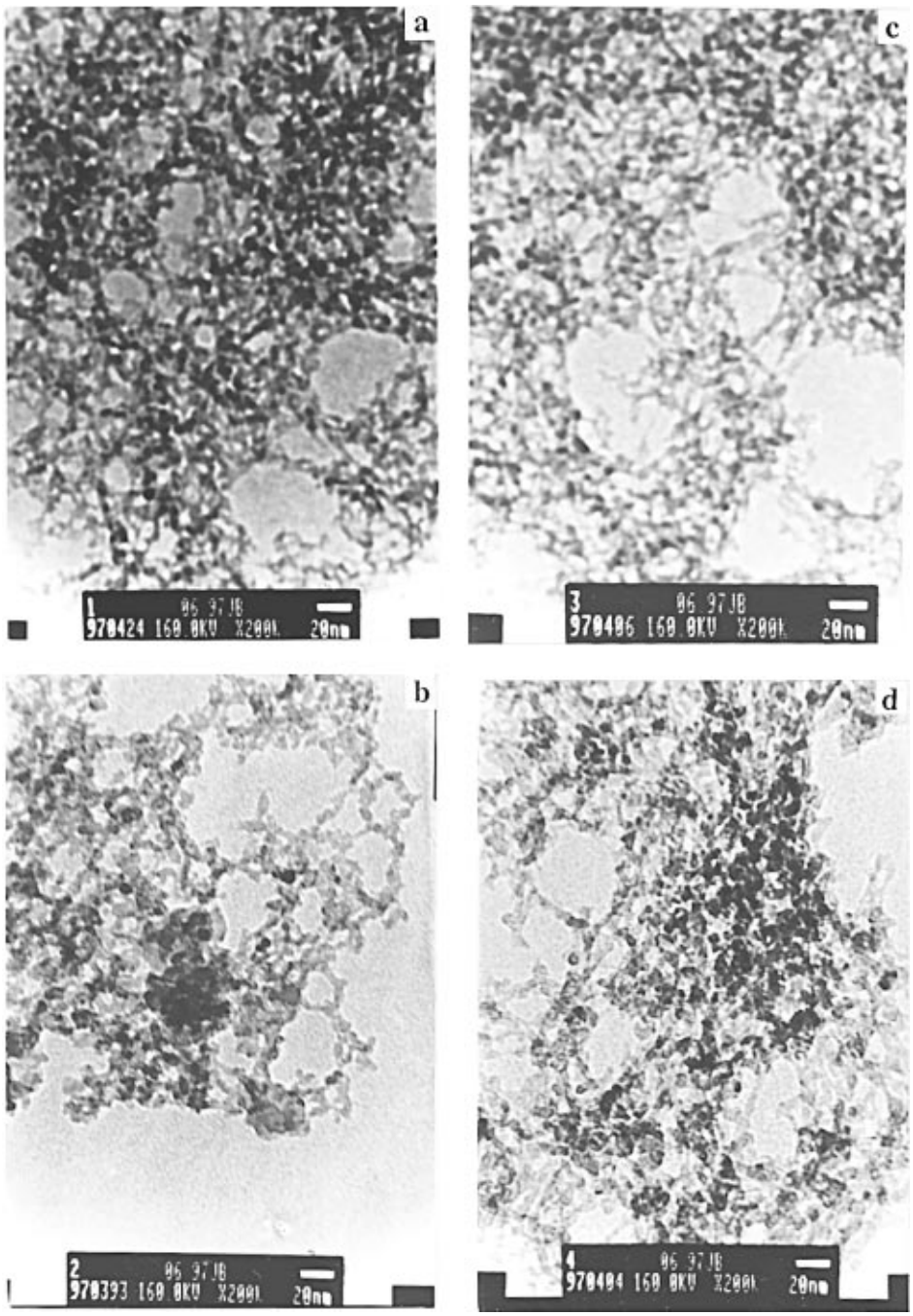

Figure 7. TEM micrographs of the samples S05A0F1.6 (a), S05A15F0 (b), F05A30F1.6 (c), and S20A0F1.6 (d).

slope of the latter curves implies a very rough surface, i.e. characterized by surface fractal dimension $D_s \gg 2$, which contrasts with the smooth surface ($D_s \simeq 2$) observed in short scales) in the former samples. In the low-**q** region (large scales) the scattering curves consistently show a power-law behavior, regardless of the catalyst used, with the values of exponent implying mass fractal structure, i.e. the scale-independent branched polymeric structure (cf., Figures 2a and 3a). However, both the value of the mass fractal dimension D_m and the range of the constant slope strongly depend on the catalyst used and/or its concentration, which clearly demonstrates a different effect of each of the catalysts. Interestingly enough, the increase in the concentration of ammonium hydroxide consistently leads to the decrease in D_m (and thus to the formation of a less ramified, sparser polymeric structure[17]) and a narrower range of mass fractality. This trend is observed in both S05 and S20 samples (see Figures 2a and 4a). In contrast, an increase in concentration of fluoride ions markedly widens the range of mass fractality but has little bearing on the value of D_m (Figure 3a). Evidently, fluoride ions strongly promote formation of a highly branched polymeric structure in the system considered. This fine polymeric structure is clearly seen in TEM images of the samples shown in Figure 7. However, differences in the morphology of the samples and the specific features detected by the scattering method are not clearly seen in the micrographs.

The irregularity of the surface geometry quantified by D_s ($2 \leq D_s < 3$) can be related to the shape of the PSD; steeper PSDs were found theoretically to induce fractally rougher surfaces.[18,19] Figure 5 presents plots of the PSDs

(17) Martin, J. E.; Hurd, A. J. *J. Appl. Crystallogr.* **1987**, *20*, 61.

(18) Jaroniec, M.; Lu, X.; Madey, R.; Avnir, D. *J. Chem. Phys.* **1990**, *92*, 7589.

(19) Jaroniec, M.; Gilpin, R. K.; Choma, J. *Carbon* **1993**, *31*, 325.

from four aerogels of the S05 series. As can be seen, a notable presence of small mesopores is detected in both samples synthesized using a single-component catalyst (higher for A15F0), while in those prepared with a larger content of the two-component catalyst the small mesopores are less numerous. The steep PSDs, recorded in the former samples in the range of small mesopores, well consort with fractally rough surfaces predicted by the slopes of the scattering curves in short scales. Similarly, more uniform PSDs from the latter samples well comply with smooth surfaces depicted by Porod law scattering (see Figures 2b and 3b). This perfectly conforms with the theory of Jaroniec et al.[18,19] The broad peaks of pores in the range 6−40 nm, observed in Figure 5, portray intracluster voids which generate mass fractality depicted by the scattering curves in the same length scales (cf., Figures 2a and 3a). This structural heterogeneity also contributes to irregularities of the internal surface structure which can be investigated by examining N_2 adsorption isotherms in light of the generalized Frenkel−Halsey−Hill (FHH) isotherm equation proposed by Avnir et al.,[20] Pfeifer et al.,[21,22] and Yin.[23] This approach has already been extensively discussed[24,25] and exploited in similar situations,[26,27] and for this reason it is not detailed here. As can be seen from Figure 6 all experimental isotherms from S05 samples indicate a fair linearity in the relative pressure range 0.4−0.95 with the absolute value of the constant slope $|1/m|$ in excess of $^1/_3$. According to Pfeifer et al.,[21] this slope implies the capillary condensation mechanism of adsorption and thus the relation $D_s = 3 - |1/m|$, which gives the values indicated in Table 1. From Figure 6 and Table 1 it can also be seen that an internal surface of aerogels is fractally rough in large scales, $D_s \simeq 2.53-2.65$, irrespective of the catalyst. However, the surface roughness of the S05A15F0 sample is higher than that observed in aerogels synthesized using mixed catalyst. Interestingly enough, the internal surface of the S05A15F0.8 aerogel appears to be the second roughest, and that of S05A0F1.6, the least rough, respectively. The above effect of the catalyst was not seen in S20 samples. In this case all isotherms overlapped in the relative pressure range 0.4−0.95 with the constant slope value corresponding to $D_s \simeq 2.6$.

The presented results clearly show that F^- and OH^- anions differently affect the process of structure formation. While fluoride anions stimulate formation of a highly ramified self-similar polymeric structure in larger-length scales, which may portray that postulated by the theory of percolation (cf. identical values of $D_m \simeq 2.5$[14b]), hydroxide anions impair this action, as can be inferred from the decrease in D_m, and promote formation of sparser, weakly branched networks. In neutral or mildly basic conditions TEOS hydrolysis is rate-limiting in the total gelation process;[28] thus, fluoride anions boost this very reaction in the first instance. Apparently, this drastically changes the conditions of gelation and renders them similar to those of the two-step acid−base-catalyzed process. A remarkable similarity of the presented morphologies with those of aerogels obtained from this two-step process[29] corroborates this view. It is noteworthy that this similarity not only covers the main features of morphology but goes even as far as the polymeric chains' thickness. Indeed, the values of l_m given in Table 1 very well conform with the 3 nm width of chains observed in two-step aerogels.[29]

Acknowledgment. The authors gratefully acknowledge the financial support of State Committee for Scientific Research (KBN) for this work under Grand 3T09C-022-09.

LA9703454

(20) Avnir, D.; Jaroniec, M. *Langmuir* **1989**, *5*, 1431.
(21) Pfeifer, P.; Cole, M. V. *New J. Chem.* **1990**, *14*, 221.
(22) Ismail, I. M. K.; Pfeifer, P. *Langmuir* **1994**, *10*, 1532.
(23) Yin, Y. *Langmuir* **1991**, *7*, 216.
(24) Jaroniec, M. *Langmuir* **1995**, *11*, 2316.
(25) Sahouli, B.; Blacher, S.; Brouers, F. *Langmuir* **1996**, *12*, 2872.
(26) Ehrburger-Dolle, F.; Holz, M.; Mauzac, C.; Lahaye, J.; Pajonk, G. M. *J. Non-Cryst. Solids* **1992**, *145*, 185.
(27) Jarzębski, A. B.; Lorenc, J.; Aristov, Yu. I.; Lisitza, N. *J. Non-Cryst. Solids* **1995**, *190*, 198.
(28) Brinker, C. J. *J. Non-Cryst. Solids* **1988**, *100*, 30.
(29) Tillotson, T. M.; Hrubesh, L. W. *J. Non-Cryst. Solids* **1992**, *145*, 44.